Evaluation of transport coefficients of simple fluids by molecular dynamics: Comparison of Green-Kubo and nonequilibrium approaches for shear viscosity

J.-P. Ryckaert and A. Bellemans
Physics Department, Université Libre de Bruxelles (Code Postal 223), Campus Plaine, boulevard du Triomphe, B-1050, Bruxelles, Belgium

G. Ciccotti
Section de Recherches de Métallurgie Physique, Centre d'Études Nucléaires de Saclay, 91191 Gif-sur-Yvette Cédex, France
and Dipartimento di Fisica Università degli Studi di Roma "La Sapienza," piazzale Aldo Moro 2, I-00185, Roma, Italy

G. V. Paolini
Dipartimento di Fisica Università degli Studi di Roma "La Sapienza," piazzale Aldo Moro 2, I-00185, Roma, Italy
(Received 6 July 1988)

Nonequilibrium molecular dynamics (NEMD) experiments measuring the shearing forces within an atomic fluid undergoing a planar Couette flow [Hoover, Ann. Rev. Phys. Chem. **34**, 103 (1983); Evans and Morriss, Comp. Phys. Rep. **1**, 299 (1984)] are performed by the subtraction method [Ciccotti *et al.*, J. Stat. Phys. **21**, 1 (1979)] at sufficiently low velocity gradient in order to remain within the linear response regime. The resulting stress averaged over many hundreds of NEMD trajectories (segments) and the stress-stress time autocorrelation function evaluated along the available equilibrium trajectory (required for the subtraction method), which are formally related by linear response theory, are shown to yield compatible estimations of the shear viscosity. This confirms the correct limiting behavior of the effective shear viscosity evaluated by similar NEMD experiments at much larger gradients. At the fluid state point far from the melting line that we consider, no size dependence of the viscosity is observed in both types of experiments. A comparison of the efficiency of both methods is not straightforward, as we found that, for a fixed number of time steps, the error estimated on the viscosity is independent of the system size for the Green-Kubo formula but decreases as $N^{-0.5}$ in the NEMD case.

I. INTRODUCTION

It is now well established that for dense fluids, the numerical evaluation of transport coefficients by molecular dynamics (MD) simulations can proceed in various ways. The exploitation of Green-Kubo (GK) relations at equilibrium (EMD) appears nowadays as the traditional "old fashioned" method, as, in the last few years, the computation of transport coefficients via direct application of the phenomenological laws in nonequilibrium MD simulations (NEMD) has become increasingly popular.[1]

For the systems accessible to simulation by computers, i.e., involving a few hundreds particles, bulk fluid-transport coefficients are more adequately obtained by methods which preserve space homogeneity[2-4] in comparison with models, closer to real experiments, where gradients are imposed by an explicit fluid-wall interaction.[5,6] In the former class of methods, a current of mass, momentum, or energy is induced throughout the system by a fictitious external field. This field is chosen in such a way that the ratio between the specific current and the field itself (i.e., the susceptibility) corresponds precisely, in the low field limit, to the transport coefficient of interest. To obtain a strictly homogeneous steady state, one introduces an additional coupling of the system to a thermostat removing uniformly the heat dissipated. The equations of motion are similar to the ones employed in EMD but contain additional external fields and thermostat coupling terms. It is useful to remind at this point that, given the high fields required to get a reasonable signal-to-noise ratio, the effective transport coefficients are field dependent so that calculations must be performed at various field strengths and subsequently extrapolated to zero field.

NEMD can, however, also be performed in a dynamic way at much smaller gradients (largely within the linear response regime) by using the subtraction method.[7] Starting from an equilibrium state, the transient behavior of a system suddenly subjected to the field (either constant or deltalike in time) is followed until a (quasi) stationary state is recovered. As the coupling is small, the response emerges out of the noise by averaging the difference between the currents measured at equivalent times along perturbed and unperturbed (no field) trajectories, starting from a common configuration. With a suitable choice of the external coupling, the response in the linear regime is related to the equilibrium current-current time correlation function of interest and therefore to the relevant transport coefficient. The NEMD equations are similar to those mentioned earlier for the none-

quilibrium steady-state simulations, except for the thermal bath coupling terms which are no longer required as heating up effects are negligible.

Such methods have been used recently by some of us in the calculation of thermal conductivity[8] and shear viscosity[9,10] using more statistics than in earlier attempts.[3] The equivalence of these methods with the corresponding usual Green-Kubo method is numerically verified, as predicted by generalized linear response theory.[11]

Nevertheless, contradictory opinions or doubts still circulate[12] about the efficiency and sometimes about the equivalence of the three different techniques recalled briefly above, i.e., (1) Green-Kubo, (2) large-gradient stationary NEMD method with extrapolation to zero gradient, and (3) the subtraction NEMD method at small (essentially zero) gradient. Careful and unambiguous intercomparison of all these methods on simple reference systems are thus required even if some studies in that direction have been published recently. Results on hard-spheres viscosity using high-gradient NEMD[13,14] and GK methods have always been found in apparent agreement. Evans and Holian[15] arrived at the same conclusion for the shear viscosity of a Lennard-Jones fluid at a supercritical state again using Green-Kubo and large-gradient stationary NEMD. In the same context, a systematic comparison of these methods, including their efficiency, has recently been published by Erpenbeck[16] for the self-diffusion coefficient of a dense liquid. Agreement between both methods is again observed but only in the large system limit (in practice for $N > 1372$), the N dependence being more pronounced in NEMD than expected. For the same given number of time steps, the GK method achieves, in this case, the best precision on the transport coefficient and is therefore considered superior to the NEMD large-gradient approach. It must be stressed, however, that this comparison of efficiency is somewhat biased by the fact that the NEMD method computes a collective quantity $\mathbf{J}=\sum_i e_i \mathbf{v}_i$ (where $\mathbf{v}_i$ is the velocity of atom i and e_i a "color label" equal to $+1$ or -1) while the EMD method evaluates directly the self-quantity $\langle \mathbf{v}_i(t)\cdot\mathbf{v}_i(0)\rangle$ which rigorously puts to zero the cross terms $\langle \mathbf{v}_i(t)\cdot\mathbf{v}_j(0)\rangle$ which would appear as a noise source in the $\langle \mathbf{J}(t)\cdot\mathbf{J}(0)\rangle$ equilibrium correlation function.

In this paper we present a systematic comparison of the GK and NEMD low-gradient (subtraction) methods for the same fluid and state point considered by Evans and Holian.[15] For reference purposes, we present some results on the heat conductivity of this system obtained by both kinds of techniques, but the paper, both in its numerical results and theoretical aspects, will otherwise be concerned exclusively with the shear-viscosity transport coefficient. These new results complement the work of Holian and Evans both by increasing GK statistics and by testing the subtraction technique as a possible NEMD alternative. In a recent paper,[10] we already reported the results of nonstationary NEMD methods (at both small and large gradients) discussing the shear-rate dependence of the viscosity for the same system (108 particles) at the same point. In that work we observed agreement between the Green-Kubo result, the zero-gradient extrapolation estimate of large-gradient NEMD results and the small-gradient (subtraction technique) result. In the present paper we focus on the low-gradient subtraction method. Looking at different system sizes and performing a detailed statistical convergence analysis, we compare the nonequilibrium results, i.e., the susceptibility to an appropriate external perturbation, to their equivalent time correlation function expressions computed along the equilibrium trajectory.

In Sec. II we describe the NEMD method devised to measure the shear viscosity of a simple fluid using a δ-type perturbation, corresponding physically to an impulsive shear of the system. The shear viscosity can be related to the relaxation to equilibrium of such externally induced shearing force.

In Sec. III we analyze shear-viscosity results obtained by both GK and NEMD techniques for three system sizes ($N=108$, 500, and 1372) and heat conductivity estimates for the 500-particle system.

Section IV deals with the statistical convergence of the two methods and the analysis of the data. The paper ends with a discussion of the drawbacks and the merits of the NEMD subtraction method.

II. THEORETICAL BACKGROUND AND IMPLEMENTATION OF NEMD

As a way to introduce useful notations, we start with the Green-Kubo expression of the shear-viscosity coefficient η,[17] used in standard EMD simulations. It involves the time correlation function of the off-diagonal elements of the stress tensor σ and for an atomic fluid of N particles occupying a volume V at temperature T,

$$\eta = \lim_{t\to\infty} \eta(t) ,$$
$$\eta(t) = (V/k_B T)\int_0^t \langle \sigma_{xy}(s)\sigma_{xy}(0)\rangle ds , \tag{1}$$

where $\langle \cdots \rangle$ denotes an equilibrium average in phase space and the stress tensor is given by

$$\sigma_{xy} = -(1/V)\sum_i (m_i^{-1} p_{ix}p_{iy} + f_{ix}y_i) ; \tag{2}$$

m_i, $\mathbf{r}_i$, and $\mathbf{p}_i$ are, respectively, the mass, Cartesian coordinate, and momentum of atom i, while $\mathbf{f}_i$ is the total force acting on this atom.

Alternatively, NEMD simulations of fluids, subject to shear flows, have been devised to get η in a more direct way.[1,2] In this case to minimize surface effects, it is preferable to choose a method preserving the spatial homogeneity of the system. The velocity gradient, induced throughout the MD cell by application of a fictitious external field, has then to be accommodated at the boundaries by appropriate generalized periodic boundary conditions. What happens to the system is easily described as a deformation of the MD cell induced by the fluid flow itself. Just as in the Parrinello-Rahman method for solid deformation under external stress,[18] the

primary cell is defined by three noncoplanar basic vectors $\mathbf{H}_1,\mathbf{H}_2,\mathbf{H}_3$ arranged as the columns of a 3×3 matrix $\mathbf{H}$ (Fig. 1): The N primary (basic) particles have reduced coordinates $\mathbf{H}^{-1}\mathbf{r}$ lying between 0 and 1 while image particles, follow as

$$\mathbf{r}_i^{\Delta}=\mathbf{r}_i+\mathbf{H}\cdot\Delta \ , \tag{3}$$

where Δ is a vector of three integer elements $\Delta_1,\Delta_2,\Delta_3$, specifying a particular replica of the primary cell, each element giving the number of elementary translations in the corresponding direction (see Fig. 1).

To impose a particular fluid flow, we resort to the so-called SLLOD equations[2]

$$d\mathbf{r}_i/dt=\mathbf{p}_i/m_i+(\nabla\mathbf{u})^{\mathrm{T}}\cdot\mathbf{r}_i \ , \tag{4a}$$

$$d\mathbf{p}_i/dt=\mathbf{f}_i-(\nabla\mathbf{u})^{\mathrm{T}}\cdot\mathbf{p}_i \ , \tag{4b}$$

where the tensor $\nabla\mathbf{u}$ is the desired spatially homogeneous velocity gradient. It is possible, quite generally, to accommodate such fluid flow at the boundaries in such NEMD simulations. To grasp the idea, it is easier to look the model fluid as an infinite periodic system throughout which an homogeneous velocity gradient is set up. Such fluid flow will at the same time deform (in a macroscopic sense) the primary cell and the image cells in such a way that periodicity is preserved. This can be verified explicitly on the basis of Eqs. (4) supposed to apply to all molecules of the infinite array. If $\mathbf{p}_i/m_i$, interpreted as the non systematic part (thermal part) of the velocity of molecule i, is taken identical for a molecule of the central cell and all its images, i.e.,

$$\mathbf{p}_i^{\Delta}=\mathbf{p}_i \quad \text{for all } \Delta \ , \tag{3'}$$

it then easily follows that relations (3) and (3') will automatically persist in time provide the box itself evolves as

$$\dot{\mathbf{H}}=(\nabla\mathbf{u})^{\mathrm{T}}\cdot\mathbf{H} \ . \tag{5}$$

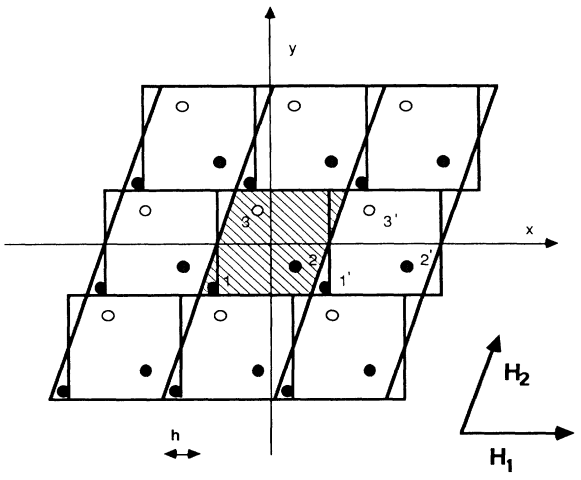

FIG. 1. Periodicity in a shear flow. The basic cell is either a parallelipipedic box (containing atoms 1, 2, and 3) or a cubic one (atoms 1', 2, and 3) with displaced cube images in the x direction (by a multiple of h) according to the y separation.

This can be shown by substitution of Eqs. (3) and (3') in Eqs. (4) written for an arbitrary molecule i in any image cell: Thanks to Eq. (5), these equations of motion reduce to those involving molecule i of the primary cell. Equation (3) with a time-dependent $\mathbf{H}$ matrix thus provides the spatial coherence of trajectories of a family of image molecules. NEMD reduces thus to the integration of $6N$ first-order differential equations (4) and to the box dynamics which is usually performed analytically. When a particle leaves the box (due to thermal motion), it reenters at the same time inside at a symmetry-related position, its linear momentum $\mathbf{p}$ being unaffected in this operation.

A usual practice[1,2] is to simulate a *stationary flow,* always chosen so far to be the simple planar Couette flow, and evaluate the shear-viscosity coefficient as the ratio of tangential stress and shear rate according to its macroscopic definition. Here, we will also consider a planar Couette flow in which the velocity field is directed along x and the system sheared perpendicularly to y. However, we adopt the special case of a δ-like perturbation in time for the field, i.e., $\nabla\mathbf{u}$ thus takes the form

$$\nabla\mathbf{u}\begin{bmatrix}0&0&0\\ h_0\delta(t)&0&0\\ 0&0&0\end{bmatrix} . \tag{6}$$

Providing the dimensionless parameter h_0 is chosen sufficiently small, generalized linear response theory (LRT)[11] then leads to

$$\langle\hat{\sigma}_{xy}(t)\rangle=h_0(V/k_BT)\langle\sigma_{xy}(t)\sigma_{xy}(0)\rangle \tag{7}$$

in which all averages are performed over equilibrium ensembles. In Eq. (7) the time evolution involves field-free equations (equilibrium trajectory) on the right-hand side (rhs) but perturbed dynamics on the left-hand side (lhs) as reminded by the caret symbol. Comparing Eqs. (1) and (7), $\eta(t)$ can thus also be estimated as

$$\eta(t)=\lim_{h_0\to0}h_0^{-1}\int_0^t\langle\hat{\sigma}_{xy}(s)\rangle ds \ . \tag{8}$$

The NEMD experiment exploits Eq. (8) by following a large number of perturbed segments $\hat{\sigma}_{xy}(t)$ over a time t^* sufficiently long for the system to come back to equilibrium (typically a few correlation times of the stress autocorrelation function). The initial conditions are generated by a standard EMD trajectory along which configurations are usually selected at equally spaced intervals t^* to guarantee the independence of the NEMD trajectories.

In order to extract a signal out of noise in the evaluation of $\eta(t)$ for the small perturbation considered, the average on the lhs of Eq. (7) must be computed as $\langle\hat{\sigma}_{xy}(t)-\sigma_{xy}(t)\rangle$, where $\sigma_{xy}(t)$ is the xy stress tensor element computed along the unperturbed trajectory starting from the same initial configuration. This subtracting term, averaging to zero, is indeed highly correlated to the NEMD response at short times. Note that this quantity is automatically provided by the EMD mother trajectory used to generate the set of initial configurations, and no extra calculations are really implied. It should be

stressed here that this subtraction technique requires a continuous force model. Use of an abrupt cutoff in the pair potential, for example, leads to unphysical peaks in $\hat{\sigma}_{xy}(t)-\sigma_{xy}(t)$ when it happens that a pair of atoms is slightly within the cutoff distance in one trajectory and slightly beyond this distance in the related segment. This can be easily avoided by smoothing artificially the discontinuity by a linear or sigmoid function.[9]

The implementation of the NEMD experiment follows usual practice,[7-9] and we will only describe here the less known effects of the δ-like perturbation [Eq. (6)] on the system and its images around time 0. Direct integration of Eqs. (4) and (5) for the specific field of Eq. (6) yields

$$\begin{aligned} &x_i(0^+)=x_i(0^-)+h_0 y_i(0^-)\ , \\ &p_{ix}(0^+)=p_{ix}(0^-)-h_0 p_{iy}(0^-)\ , \\ &y_i(0^+)=y_i(0^-),\quad p_{iy}(0^+)=p_{iy}(0^-)\ , \\ &z_i(0^+)=z_i(0^-),\quad p_{iz}(0^+)=p_{iz}(0^-)\ , \end{aligned} \tag{9a}$$

$$\mathbf{H}(0^+)=\begin{vmatrix} 1 & h_0 & 0 \\ 0 & 1 & 0 \\ 0 & 0 & 1 \end{vmatrix}\mathbf{H}(0^-)\ . \tag{9b}$$

As usual, the MD primary cell is supposed to be cubic at equilibrium with side L, so that $\mathbf{H}(0^+)$ takes the particular form

$$\mathbf{H}(0^+)=\begin{vmatrix} L & h_0 L & 0 \\ 0 & L & 0 \\ 0 & 0 & L \end{vmatrix}\ . \tag{10}$$

NEMD trajectories are thus produced by applying to the system its instantaneous modification [Eqs. (9a) and (10)], followed by a field-free usual MD. The only unusual element in this dynamics is the nonorthorombic character of the unit cell implying a slightly more complicated search of a closest-image atom in the force calculation, even if, for a parallelipipedic box not too far from orthogonality, this search can sometimes be performed as usual if reduced coordinates are used. For details, we refer to the Parrinello-Rahman method[8] where the identical problem is encountered. In the particular case of the simple planar Couette flow, the quasi-infinite system considered in the simulations can be viewed in a well-known alternative way, originally suggested by Lees and Edwards (LE) (Ref. 4) to accommodate a stationary flow of this type in MD simulations. Relative to our general approach [Eqs. (3)–(5)], the LE picture can be reconstructed at any time by redefining the set of atoms explicitly followed as those lying inside the unaltered original cubic box which is thus kept fixed in space. The infinite system is then reconstructed at any time by translational symmetry operations [Eq. (4)] based on the same matrix $\mathbf{H}(t)$, solution of Eq. (5) but which, strictly speaking, has lost its MD box interpretation (see Fig. 1). The picture now consists of an arrangement of displaced cubic bricks as each cell, with respect to its original location, has been displaced in the x direction proportionally to y as a result of the velocity field. For a stationary planar Couette flow, the usual sliding-bricks picture of Lees-Edwards is recovered. For the present impulsive field [Eq. (6)], the displacement of the image cells is frozen once the perturbation is over. On the basis of $\mathbf{H}(0^+)$ [Eq. (10)], the displacement of an image cell defined by $(\Delta_1,\Delta_2,\Delta_3)$ [see Eq. (3)] is equal to $\Delta_2 h_0 L$ in the x direction (Fig. 1 with $h=h_0 L$).

For its somewhat greater simplicity in the search of atomic pairs lying within a given radius of interaction, our program follows the second method. For an initial equilibrium configuration consisting of N atoms enclosed in a cubic cell, the explicit treatment around $t=0$ consists finally in (a) applying Eq. 9(a) to all atoms and (b) resetting the coordinate of any atom lying now outside (as a result of the perturbation) by the one of the corresponding image having entered the box through the opposite side. During the following dynamics, the search for the closest image of an atom j with respect to an atom i located in the primary cubic box requires the minimization with respect to $\Delta_i, i=1,3$ of the distance

$$|\mathbf{r}_j-\mathbf{r}_i|=|\mathbf{r}_j+(\Delta_1+h_0\Delta_2)L\boldsymbol{l}_x+\Delta_2 L\boldsymbol{l}_y+\Delta_3 L\boldsymbol{l}_z-\mathbf{r}_i|\ ,$$

where $\boldsymbol{l}_x$, $\boldsymbol{l}_y$, and $\boldsymbol{l}_z$ are unit vectors pointing along the three sides of the cubic box. These integers are obtained by first determining Δ_2 and Δ_3 by the usual procedure minimizing the y and z component of the interatomic vector. The x component of the same vector is then minimized on Δ_1 for fixed Δ_2.

III. DESCRIPTION AND RESULTS OF MD EXPERIMENTS

We are studying a simple fluid of N atoms interacting via a pairwise additive potential based on the Lennard-Jones (LJ) pair interaction $v(r)$ truncated at its inflexion point $r_c=(\frac{26}{7})^{1/6}$ by a cubic spline reaching 0 smoothly (tangentially) at $r_m=\frac{67}{48}r_c\approx 1.74$. Lengths, and in the following all quantities, are quoted in reduced units based on the mass of an atom m and the LJ σ and ϵ parameters. In explicit form, this potential, proposed by Holian and Evans,[15] reads

$$\begin{aligned} &v(r)=4(r^{-12}-r^{-6})\quad \text{for } r<r_c\ , \\ &v(r)=\tfrac{7}{61\,009}[67-48(r/r_c)]^2[5-24(r/r_c)] \\ &\qquad\qquad \text{for} r_c<r<r_m\ , \\ &v(r)=0\quad \text{for } r>r_m\ . \end{aligned} \tag{11}$$

It offers two advantages with respect to the usual LJ interaction which is usually truncated at a cutoff distance between 2.5 and 3.0. (i) Its derivative is continuous, a property which facilitates the application of our NEMD method at small gradient, and (ii) it has quite a shorter range so that the calculation of the forces at each step is more efficient. At the same time, this model was precisely the object of a comparison between EMD and the large-gradient stationary NEMD methods in the compu-

tation of the shear viscosity, and for this reason, we performed our own calculations at the same state point considered, a supercritical point of density $\rho=0.7$ and temperature $k_BT=2.75$.

In this paper our aim is to compare the two very different methods to compute the function $\eta(t)$ [Eqs. (1) and (8)], the asymptotic limit of which determines the zero-shear-rate viscosity η. Let $\bar{\eta}(t)$ represent the estimate of $\eta(t)$ using Green-Kubo formula [Eq. (1)] applied to the EMD mother trajectory of the nonequilibrium experiment and $\hat{\eta}(t)$ the corresponding estimate obtained through Eq. (8) according to the low-gradient NEMD technique (linear regime) described in Sec. II. Molecular dynamics experiments were performed for different system sizes ($N=108$, 500, and 1372) using the velocity version of the Verlet numerical integration algorithm with $\Delta t=0.005$.[19] The length of all experiments is mentioned in Table I. Note that, as the length of a NEMD trajectory, on the one hand, and the time interval between two consecutive NEMD initial configurations along the equilibrium path, on the other hand, are both taken equal to 150 time steps ($t^*=0.75$), the total number of MD steps

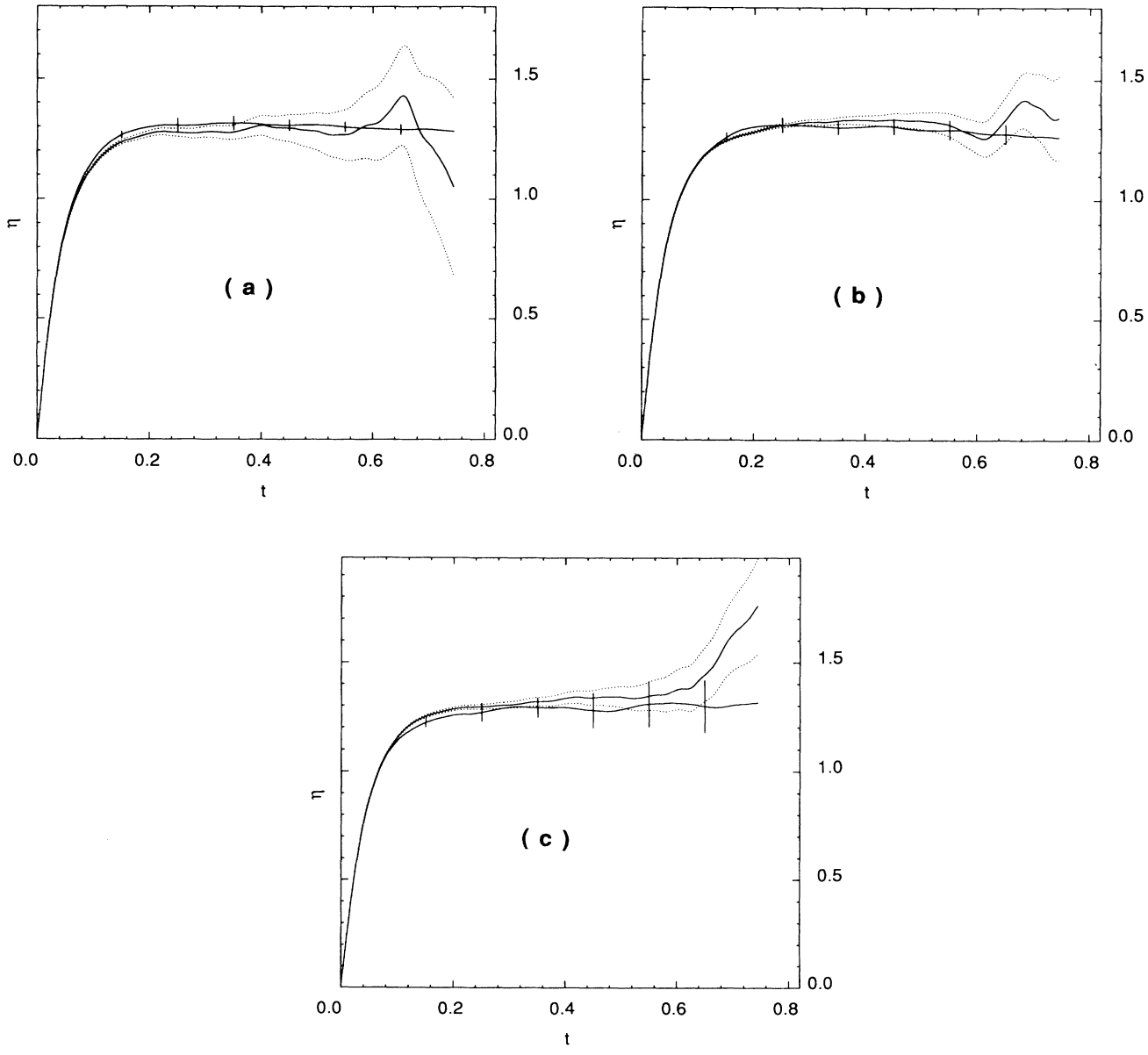

FIG. 2. Running time integral of the stress-stress autocorrelation function (properly scaled to yield η asymptotically) obtained by the direct Green-Kubo equilibrium method (solid curve with error bars) and by the trajectory NEMD method (solid curve with standard deviation indicated by dotted curves) (a) $N=108$, (b) $N=500$, and (c) $N=1372$. (All units are usual reduced units; see text.)

TABLE I. List of experiments and main results. Shear viscosity η and heat conductivity λ of the Lennard-Jones fluid (pair potential truncated at $r=1.74$) evaluated by Green-Kubo and NEMD subtraction technique. Errors are estimated as one standard deviation of subexperiments results.

EMD experiments				
N	No. of steps	k_BT	η	λ
108[a]	19 500	2.75	1.26±0.08	
108[b]	210 000	2.753	1.30±0.02	
108[b,c]	970 000	2.753	1.29±0.01	
500[a]	18 000	2.75	1.24±0.07	
500[b]	210 000	2.758	1.30±0.04	
500[b]	180 000	2.75		5.9±0.2
1372[b]	45 000	2.755	1.275±0.10	
4000[a]	9000	2.74	1.35±0.16	
NEMD experiments				
N	No. of trajectories		η	λ
108[b]	1400		1.28±0.03	
500[b]	1400		1.30±0.01	
500[b]	1200			5.55±0.05
1372[b]	300		1.30±0.01	

[a]Reference 15.
[b]Our results.
[c]The first 210 000 steps of the trajectory of this experiment are identical to those used in the previous line.

performed along both kinds of trajectories is identical. For $N=108$ a much longer EMD run was also available.

In the nonequilibrium method, a value of $h_0=10^{-6}$ was adopted for the perturbation. However, it turns out that individual segments $[\hat{\sigma}_{xy}(t)-\sigma_{xy}(t)]/h_0$ are independent of h_0 until the time limit t^*, provided h_0 lies below $h_{\max}=10^{-3}$ but above a minimal value sufficiently large to avoid significative round-off errors in the subtraction. Such mechanical linearity implies the required statistical linearity as the average in the rhs of Eq. (8) is performed over an equilibrium ensemble.

In Fig. 2 [(a)–(c) for $N=108$, 500, and 1372], $\bar{\eta}(t)$ and $\hat{\eta}(t)$ are shown with associated uncertainties. The agreement of the two approaches is clearly apparent with a plateau emerging much before t^* from both curves for each system size. This plateau value is fixed by a systematic fitting procedure assuming an exponential evolution of $\eta(t)$ towards its asymptotic limit. In Sec. IV we will explain the method used to analyze the data. Results concerning η are given in Table I. The relaxation time τ is always found close to 0.05. In the table we also mention Holian and Evans EMD results[15] which are consistent with ours. Here again, EMD and NEMD estimates of the transport coefficient appear to agree perfectly with each other.

Quite interestingly, our results do not suggest any size dependence of η, regardless of which method is used. This might not be true at state points closer to the melting line, where this dependence has been for many years the object of some controversy.[20–23]

In Table I we also report compatible values of the heat conductivity λ computed by Green-Kubo[17] and NEMD subtraction method[24,25,8] for the same fluid. The agreement is reasonable as error bars are only one standard deviation.

IV. STATISTICAL CONVERGENCE OF BOTH METHODS

The observed agreement on $\eta(t)$ between results obtained by EMD and low-perturbation NEMD techniques is not really a surprise as both methods rely on two theoretically equivalent formulations [Eqs. (1), (2), (7), and (8)].

The statistical convergence of the two methods is not the same, however, as the EMD experiment probes natural fluctuations of the system while the NEMD one follows the decay of artificially induced fluctuations. The contrast is best illustrated by the striking difference in the time evolution of the standard deviation on the mean $\eta^*(t)$ estimated by the standard formula

$$\Delta\eta(t)=\left[\sum_k [\eta_k(t)-\eta^*(t)]^2/[N_{\text{expt}}(N_{\text{expt}}-1)]\right]^{1/2} \tag{12}$$

based on N_{expt} independent estimates $\eta_k(t)$. In the EMD case, $\Delta\bar{\eta}(t)$ is based on N_{expt} partial Green-Kubo subexperiments averages $\tilde{\eta}(t)$ while in the NEMD case, N_{expt} is the total number of trajectories $\eta'(t)=[\hat{\sigma}_{xy}(t)-\sigma_{xy}(t)]/h_0$. For any system size, $\Delta\bar{\eta}(t)$ does not change in a significant way beyond $t=0.2$, at least over the period of time investigated while $\Delta\hat{\eta}(t)$ (see Fig. 3) increases exponentially for $t>0.2$ as a consequence of

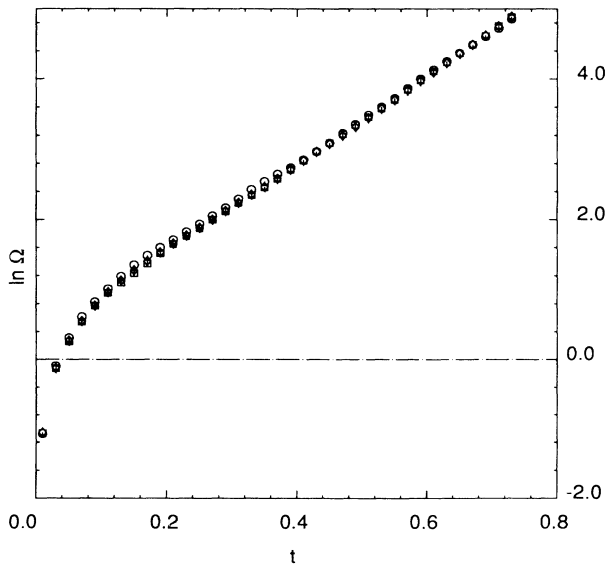

FIG. 3. Exponential divergence in time of the error $\Delta\hat{\eta}(t)$ and its system size dependence illustrated by the common behavior in time of $\ln\Omega$ with $\Omega(t)=\Delta\hat{\eta}(t)N^{1/2}N_{\text{seg}}^{1/2}$, for all nonequilibrium experiments (□, $N=108$; ◇, $N=500$; ○, $N=1372$). (All units are usual reduced units; see text.)

the well-known divergence in phase space of two trajectories starting from arbitrarily close initial conditions. Attempts to overcome this problem have been unsuccessful up to now.[26]

The size dependence of the error is also totally different in both methods. In the EMD method, the error on the autocorrelation function of a collective intensive variable is expected to be size independent and decreases as $T^{-1/2}$ with the total time T of the experiment. This has been already verified numerically.[21] Taking into account of the roughness of such error estimates, our results corroborate this expectation [see Fig. 2 or the error estimation on η itself (Table I) computed from the plateau value of $\bar{\eta}(t)$]. For the NEMD trajectory method, Fig. 3 clearly demonstrates that the error on $\hat{\eta}(t)$ scales as

$$\Delta\hat{\eta}(t)=\gamma N^{-1/2}N_{\rm seg}^{-1/2}[\exp(t/\tau')-1]\ , \tag{13}$$

where $N_{\rm seg}$ is the number of segments and γ and τ' two parameters which turn out to be in the present case 1.492 and 0.163, respectively. Equation (13) implies that the dispersion of individual segments around the mean decreases as the number of atoms in the system increases. This can be intuitively understood in the following way: The NE experiment follows the volume average of the local tangential stress component ($k=0$ Fourier component) in a system initially sheared homogeneously. The observed size dependence simply reflects that, at the present state point, the extent ξ of spatial correlations of the local stresses fluctuations (around their nonequilibrium mean) is smaller than half the smallest MD box edge considered, i.e., $\xi<\frac{1}{2}(\frac{108}{0.7})^{1/3}=2.7$. In other words, for each NE segment, the average stress evaluated for each cubic subvolume of side length 2.7 contributes almost independently to the total volume average. The totally different size dependences of the error on $\eta(t)$ evaluated by either method is obviously an important point in the comparison of their efficiency, a point to which we will come back in Sec. V.

We now discuss the method adopted for determining the asymptotic plateau value of $\eta(t)$ on the basis of the information described previously and shown for all experiments in Fig. 2. In the following we will assume, as Fig. 2 strongly suggests, that the relevant $\eta(t)$ function has essentially reached its asymptotic limit below our NEMD time limit t^* in the sense that $[\eta(t^*)-\eta]/\eta$ is much smaller than the error of statistical origin. This restriction does not favor any one of the two methods even if in practice t^* can be established more easily *(a posteriori)* in the EMD method when the recorded stress history is available. In NEMD the choice of the length of NEMD trajectories t^* must be made at the beginning of the experiment on intuitive grounds: The choice of a too-short t^* is impossible to repair without totally redoing the experiment,[9] while too-long NEMD segments are just a waste of computing time.

The data indicate that the logarithm of the stress autocorrelation function plotted versus time is linear for $t>0.05$. Accordingly, we performed a weighed least-square fit of $\eta(t)$ in the time interval [0.05,0.75] by the two-parameters function $\eta[1-\exp(-t/\tau)]$ using a weight $\omega(t)\approx[\Delta\eta(t)]^{-2}$. The estimation of the accuracy on the η parameter in Table I is based on the dispersion of values yielded by a similar fitting analysis on subexperiments obtained by splitting an actual experiment into parts: The weight was taken uniform for each EMD partial calculation but based as before on the dispersion of individual trajectories for a NEMD subexperiment. We verified that no significative improvement results from the use of more elaborate fitting procedures and, in particular, there is no indication of an algebraic decay of the stress autocorrelation. It must be noted that this situation is certainly more favorable than in many other cases.[9] The present simple-fluid supercritical state point has been purposely chosen to make the purely statistical comparison of the two methods more transparent.

In the EMD case the error on η turns out to be equivalent, quite normally, to the typical error bar on the plateau (Fig. 2). The plateau values obtained from the NEMD curves turn out to be mainly determined by the curvature region preceeding the plateau itself as a result of the highest precision of $\eta(t)$ in that region. The much-better reproductibility of the asymptotic evolution towards the plateau in the NEMD subexperiments explains, for example, the higher precision of η obtained in the $N=1372$ case with respect to the EMD result. This result is illustrated in Fig. 4 which shows the dispersion of subexperiment averages in both types of experiments. A similar behavior was noticed in similar calculations on *n*-butane.[9]

As a final illustration of the statistical convergence of the response measured by the subtraction technique, the partial average of $\eta(t)$ for an increasing number of segments is presented in Fig. 5 where the onset of the plateau can clearly be observed.

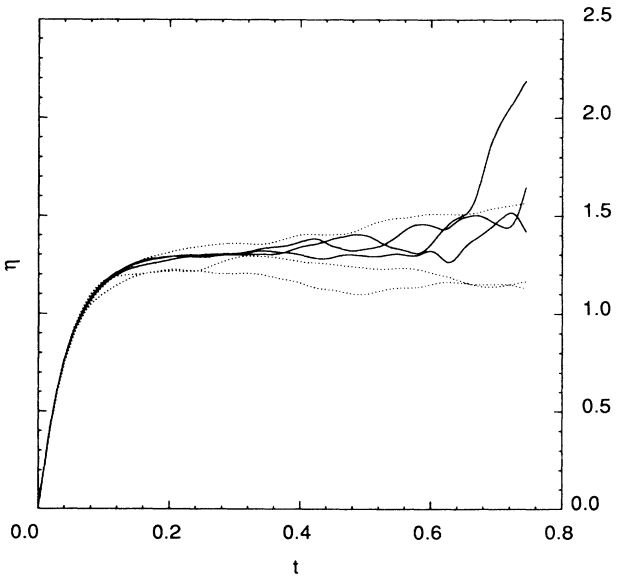

FIG. 4. Partial results for the $N=1372$ particles case. Each curve corresponds to $\frac{1}{3}$ of the statistics of (i) NEMD $\hat{\eta}(t)$ (solid curves) and (ii) Green-Kubo $\bar{\eta}(t)$ (dotted curves). All units are usual reduced units; see text.

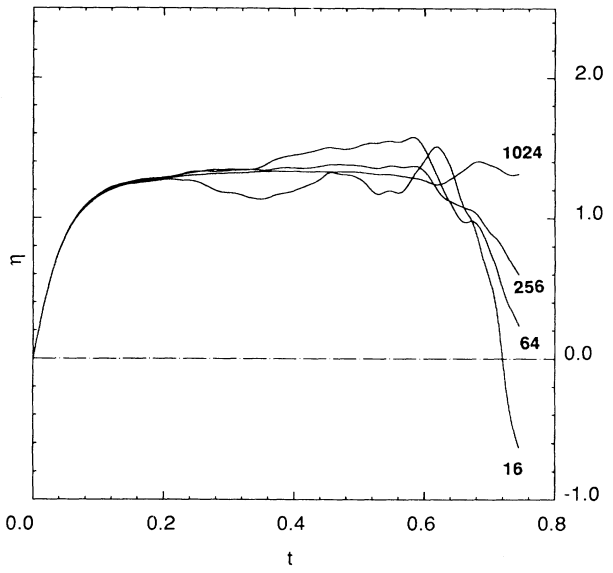

FIG. 5. Statistical convergence of the mean response $\hat{\eta}(t)$ towards a plateau behavior for the 500-particles NEMD experiment. The number of segments included in the average is indicated next to the corresponding curve. (All units are usual reduced units; see text.)

V. FINAL DISCUSSION

The results presented in this paper provide, if necessary, additional evidence on the equivalence of the equilibrium Green-Kubo approach and the subtraction NEMD trajectory method.

We are here more concerned by the comparison of the statistical convergence of these two methods in the determination of transport coefficients, in particular, the shear viscosity. This coefficient is estimated as the long-time asymptotic limit of the function $\eta(t)$ corresponding theoretically to the running time integral of the stress time autocorrelation. As already observed,[9] at short times, the error on the function $\eta(t)$ is always smaller in the NEMD response, but at longer times there is an inversion in favor of Green-Kubo results. Because only the NEMD error is size dependent, the time at which this inversion occurs is shifted towards higher values when larger systems are considered.

More generally, in comparison with the well-known EMD method, the differential NEMD technique used in the present work has both drawbacks and advantages.

In the first category, we can mention the following. (a) While all transport coefficients expressible as Green-Kubo formulas can be extracted from a single equilibrium trajectory, each coefficient requires a specific NEMD simulation experiment. The possibility of combining various fields is, however, in principle possible, as, in the linear regime, the response should be the linear combination of the effects caused by fields applied individually. (b) The error on the average response in time is growing exponentially so that it is difficult to locate the establishing of the plateau. The interpretation as noise or as a real effect of an oscillation after the onset of a first plateau, for example, is difficult.

However, many advantages of the method can be invoked. (a) It is easy for a new experiment to predict, on the basis of a few segments, the number of segments or the system size required to achieve a given accuracy [Eq. (13)]. (b) For systems of more than a few hundred molecules, the computer time, obviously proportional to the total number of segments, becomes also linear in N. Given that the same statistical improvements results in NEMD from increasing the number of particles N or the total number of segments, it is never a loss to consider a very large system: on the contrary, the gain is that significative finite system errors on the transport coefficient itself might be avoided in this way. In Green-Kubo calculations computer time is minimized by choosing the smallest possible system size. This is certainly not easy to decide *a priori*.

Our final comment will be that finally both methods are complementary more than contradictory. The possibility of obtaining information on the same quantity by two almost completely independent methods is always a reassuring fact. The difference in the time evolution of the error on the correlation function obtained by both methods could also be exploited to combine both estimates with proper weights to get the optimum precision at each time. In any case, the use of the subtraction technique also yields easily the Green-Kubo result from the EMD mother trajectory.

For completeness, it should be noted that a new method[27] (transcient correlation method) has recently been proposed to study of the shear rate dependence of the viscosity. In the context of the present paper restricted to the linear response regime, this new technique would involve in the practice the evaluation of the stress-stress time correlation function at equilibrium. Therefore, its performances should be equivalent to those of the Green-Kubo method discussed above.

ACKNOWLEDGMENTS

We thank the European Economic Community for financial support (Contract No. ST2J-0094-3-B) and the Cray Group of Statistical Mechanics, CNR, for computing facilities.

[1]W. G. Hoover, Ann. Rev. Phys. Chem. **34**, 103 (1983).
[2]D. J. Evans, and G. P. Morriss, Comp. Phys. Rep. **1**, 299 (1984).
[3]K. Singer, J. V. L. Singer, and D. Fincham, Mol. Phys. **40**, 515 (1980).
[4]A. W. Lees and S. F. Edwards, J. Phys. C **5**, 1921 (1972).
[5]W. G. Hoover and W. T. Ashurst, in *Theoretical Chemistry, Advances and Perspectives,* edited by H. Eyring and D. Henderson (Academic, New York, 1975), Vol. 1, p. 1.
[6]G. Ciccotti and C. Trozzi, Phys. Rev. A **29**, 916 (1984).
[7]G. Ciccotti, G. Jaccucci, and I. R. McDonald, J. Stat. Phys. **21**, 1 (1979).

[8]C. Massobrio and G. Ciccotti, Phys. Rev. A **30**, 3191 (1984); G. V. Paolini, G. Ciccotti, and C. Massobrio, Phys. Rev. A **34**, 1355 (1986).
[9]G. Marechal, J. P. Ryckaert, and A. Bellemans, Mol. Phys. **61**, 33 (1987).
[10]J. P. Ryckaert, A. Bellemans, G. Ciccotti, and G. V. Paolini, Phys. Rev. Lett. **60**, 128 (1988).
[11](a) D. J. Evans, in *Molecular Dynamics Simulation of Statistical Mechanics Systems, Proceedings of the International School of Physics "Enrico Fermi," Course XCVIII, Varenna, 1985,* edited by G. Ciccotti and W. G. Hoover (North-Holland, Amsterdam, 1986), p. 221; (b) D. J. Evans, Phys. Lett. **91A**, 457 (1982).
[12]H. Hanley, in Ref. 11(a), p. 317.
[13]T. Naitoh and S. Ono, Phys. Lett. **57A**, 448 (1976); J. Chem. Phys. **70**, 4515 (1979).
[14]J. J. Erpenbeck, Physica **118A**, 144 (1983).
[15]B. L. Holian and D. J. Evans, J. Chem. Phys. **78**, 5147 (1983).
[16]J. J. Erpenbeck, Phys. Rev. A **35**, 218 (1987).
[17]J. P. Hansen and I. R. McDonald, *Theory of Simple Liquids* (Academic, New York, 1976).
[18]M. Parrinello and A. Rahman, Phys. Rev. Lett. **45**, 1196 (1980).
[19]W. C. Swope, H. C. Andersen, P. H. Berens, and K. R. Wilson, J. Chem. Phys. **76**, 637 (1982).
[20]W. G. Hoover, D. J. Evans, R. B. Hicknam, A. J. C. Ladd, W. T. Ashurst, and B. Moran, Phys. Rev. A **22**, 1690 (1980).
[21]D. Levesque, L. Verlet, and J. Kurkijarvi, Phys. Rev. A **7**, 1690 (1973).
[22]M. Shoen and C. Hoheisel, Mol. Phys. **56**, 653 (1985).
[23]D. Levesque and L. Verlet, Mol. Phys. **61**, 143 (1987).
[24]D. J. Evans, Phys. Lett. **81A**, 457 (1982).
[25]M. J. Gillan and M. Dixon, J. Phys. C **16**, 869 (1983).
[26]G. Ciccotti, W. G. Hoover, C. Massobrio, and G. V. Paolini, Phys. Rev. A **36**, 3471 (1987).
[27]G. P. Morriss and D. J. Evans, Phys. Rev. A **35**, 792 (1987).